Characterizing the flavor profiles of *Linjiangsi* broad bean (*Vicia faba L.*) paste using bionic sensory and multivariate statistics analyses based on ripening time and fermentation environment

Chunyuan Ping [a,b], Xiaoqing Deng [a,*], Ziyuan Guo [a,c], Wen Luo [a], Xiang Li [a], Songlin Xin [a]

[a] *College of Culinary Science, Sichuan Tourism University, 610100 Chengdu, China*
[b] *School of Food Science and Technology, Henan Institute of Science and Technology, Henan, 453003, China*
[c] *College of Food Science and Nutritional Engineering, China Agricultural University, Beijing 100083, China*

A B S T R A C T

The flavor profile of *Linjiangsi* broad bean paste (LBBP) is significantly influenced by fermentation environment and ripening time. This study aims to investigate the flavor of outdoor-treated (OT) and indoor-treated (IT) LBBP. Gas chromatography-mass spectrometry, electronic-nose, and electronic-tongue, combined with multivariate statistical analyses, were employed to identify the characteristic flavor profiles of OT and IT LBBP in ripening periods of one and three years. Overall, 95 volatile organic compounds (VOCs) were identified. Relative odor activity values and multivariate statistical analysis indicated that nine VOCs were responsible for the flavor differences. The most abundant VOCs in OT were aldehydes, providing caramel and nutty flavors, whereas the most abundant compounds in IT were esters, contributing fruity flavors to LBBP. Notably, three years of ripening significantly intensified the characteristic flavors of both OT and IT. These findings may elucidate the ripening time and fermentation environment effect on LBBP characteristic flavor profiles.

1. Introduction

Linjiangsi broad bean (*Vicia faba L.*) paste (LBBP)—known for its high vegetable protein content and unique fermentation flavor—is widely used as a condiment across Asia. It is gaining increasing global recognition owing to its savory umami taste and significant nutritional benefits (Steinhaus & Schieberle, 2007). The fermentation process involves the microbial breakdown of complex organic compounds into simpler molecules, enhancing nutrition and providing various physiological benefits. These benefits include antioxidant and antitumor activities, hypoglycemic effects, plasma cholesterol diminution, hypotensive properties, and other documented health-protective advantages (Rai et al., 2017; Sanjukta & Rai, 2016). LBBP differs from traditional *Pixian* broad bean paste mainly because it is made from raw broad beans without boiling or steaming. This processing technique is advantageous for preserving flavor and nutritional value. Thermal processing can further damage the tissue structure of broad beans, exposing

macromolecular proteins more easily, thereby leading to the dissolution of soluble nutrients. Consequently, proteins undergo denaturation and degradation. Additionally, thermal processing can destroy heat-sensitive flavor precursors, such as amino acids and vitamins, thereby diminishing the flavor intensity of broad bean paste (Bleicher et al., 2022; Pei et al., 2023).

Flavor quality significantly influences consumer preferences, acceptance, and purchase decisions (Diez-Simon et al., 2020). Therefore, producing LBBP with a favorable flavor profile is crucial to manufacturers and researchers. Volatile organic compounds (VOCs) in traditional fermented broad bean condiments are mainly detected via the sense of smell. They include substances such as alcohols, acids, esters, aldehydes, ketones, phenols, and olefins (Li et al., 2016). However, the compositions and formation of these flavors are highly complex. Environmental conditions (outdoor or indoor) and the fermentation period are two critical factors influencing flavor compound formation. Previous studies show that environmental factors significantly affect the flavor

---

characteristics of fermented foods. Zhao et al. (2022) suggest that sunlight exposure may enhance the accumulation of volatile compounds that impart roasted aromas during fermentation. In the fermentation of broad bean paste, exposure to sunlight and air is preferred, as it contributes to a balanced flavor profile. The fermentation period is critical in ensuring fermented food quality, influencing the texture, flavor, and appearance of the final products (Sanjukta & Rai, 2016). Lu et al. (2020) found that the ripening process plays a significant role in the accumulation of key flavor compounds essential for the flavor of the final product. Their results showed that a longer ripening period led to a greater diversity of volatile compounds. Additionally, the prices of fermented products vary depending on the duration of fermentation; older fermentations result in higher prices, which may correlate with the types of volatile compounds produced during the fermentation process.

VOCs have been analyzed to understand the flavor characteristics of traditional fermented foods. Headspace gas chromatography–mass spectrometry (HS-GC–MS) is commonly employed for evaluating VOCs in traditional fermented foods such as Chinese horse bean-chili paste (Lu et al., 2020), soy sauce (Gao et al., 2017), and kimchi (Seo et al., 2018). An electronic nose (E-nose) is an array-based sensory system equipped with a suite of broadly responsive sensors, utilizing advanced signal-processing algorithms that incorporate pattern recognition and multi-variate data analysis techniques (Ma et al., 2023). Similarly, the electronic tongue (E-tongue) operates as an artificial intelligence tool for simulating the human gustatory system, capable of identifying and distinguishing complex flavors in different samples (Baldwin et al., 2011). The synergy between E-nose and E-tongue technologies has been increasingly employed in flavor analysis of fermented foods. This includes fermented shrimp paste (Deng et al., 2022), stinky tofu brine (Wang et al., 2020), Korean fermented soybean pastes (Jung et al., 2017), and other fermented foods, enabling comprehensive sensory profiling.

Despite extensive research on the flavor of broad bean paste, studies on LBBP under varying ripening times and ambient environments (outdoor- and indoor-treated) are limited. LBBP exposed to outdoor and indoor conditions over ripening periods of one and three years was explored in this study employing HS-GC–MS and bionic sensory techniques to investigate the influence of ripening time and fermentation environment on the flavor of LBBP. Therefore, this study aims to elucidate the effect of varying ripening durations and fermentation environments on the characteristic flavor profiles of LBBP. Furthermore, it seeks to provide strategic insights into the advancement and modernization of LBBP production processes.

2. Material and methods

2.1. Sample preparation

LBBP samples from three randomly selected post-fermentation batches were obtained from the *Linjiangsi* Douban Factory in Ziyang, China. This factory produces LBBP using outdoor-treated (OT) and indoor-treated (IT) methods with fermentation periods of one and three years. The specific environmental conditions of OT sample: The sample was placed in an outdoor environment and naturally ripened at ambient temperature to produce the LBBP sample. It was stirred for 30 mins once every 12 h. OT was exposed to air during both day and night, except on rainy days when it was covered. For the IT sample: The sample was ripened in an indoor environment at 32 °C with humidity exceeding 90%. The bucket cover was kept closed during fermentation to prevent sunlight exposure. IT was stirred for 30 mins once every 12 h.

For one year of ripening time: LBBP fermentation in the IT and OT group were conducted for one year, from December 17, 2022, to December 20, 2023. For three years of ripening time: LBBP fermentation in the IT and OT group were conducted for three years, from December 20, 2020, to December 20, 2023. The samples were labeled OT3, OT1, IT3, and IT1, respectively. In the OT group, LBBP fermentation was

conducted in an outdoor environment (outdoor fermentation); OT1, and OT3 represent ripening of 1 year and 3 years in outdoor environment respectively. In the IT group, fermentation was conducted in a sheltered environment (indoor fermentation); while IT1, and IT3 were represents ripening 1 year and 3 years in indoor environment respectively.

The sampling method was adopted from Liu et al. (2020) with slight modifications. The materials were completely mixed in the fermenters before being divided into three equal layers based on height. Samples from each layer were collected using a five-point sampling method. One sample was collected from the midpoint of the plane as the central point, and four additional samples were collected at equal distances along the diagonals from the midpoint. Subsequently, they were mixed evenly. The samples were immediately transported to the laboratory in a refrigerated box maintained at temperatures between −30 °C and − 55 °C. They were stored at −80 °C and analyzed within 3 days.

2.2. Evaluation of flavor sensory characteristics

A panel of trained sensory assessors, consisting of five males and five females without any documented oral or olfactory impairments, convened to evaluate the organoleptic properties of the LBBP samples from the four distinct groups. Before the assessment, the panelists were acclimated to the characteristic aromas of LBBP—including roasted, caramel, fruity, grassy, floral, nutty, and pineapple —to enhance the development of a nuanced aroma profile of the product. Sensory evaluation commenced once the panel achieved a recognition accuracy exceeding 95% for the aromas. The assessment was conducted at ambient temperature (20–25 °C), involving the presentation of 20 g samples from each group in standardized 20 mm × 20 mm glass containers. The evaluation protocol was divided into two 15-min sessions, separated by brief intermissions (5–10 min) to prevent olfactory fatigue. The weights for "taste", "appearance", "aroma", and "texture" were determined based on a pre-experiment and consensus among our sensory assessors. Table S1 shows the sensory evaluation criteria, along with their respective weights for taste (0.3), appearance (0.2), aroma (0.3), and texture (0.2). For the taste evaluation: assessors evaluated taste attributes (umami, spicy and savory) based on standardized protocols. For the appearance evaluation: Assessors rated appearance attributes (color, gloss, uniformity) using visual inspection. For the aroma evaluation: Descriptive analysis sessions where assessors described aroma attributes (fruity, floral, pineapple, nutty, roast). For the texture evaluation: Assessors chewed and touched the sample and evaluate attributes (softness, hardness, roughness, stickiness).

2.3. Determination of nutritional analysis

Compositional analysis of LBBP, including the determination of energy, protein, fat, carbohydrate, and water content, was performed using a CA-HM Food Calorimetric Component Analyzer (JWP, Tokyo, Japan). The analytical procedure was performed in quintuplicate, with each sample undergoing three measurements. The reported values for each parameter represent the mean of these independent assessments, ensuring the reproducibility of the results.

2.4. Analysis of electronic tongue

Comprehensive taste profiling was conducted using an e-tongue system (ASTREE II system, Alpha MOS Company, Toulouse, France). This device was equipped with five electrodes, each attached to a specific gustatory element: sourness (AHS), saltiness (CTS), umami (NMS), sweetness (ANS), and bitterness (SCS). For the analysis, 50 g of LBBP was mixed with 200 g of deionized water and subjected to ultrasonic agitation at 55 kHz for 25 min. The resulting solution was then filtered, and 80 mL of the clear supernatant was transferred into a 120 mL testing vessel. The e-tongue was programmed to evaluate each sample for 120 s. To maintain consistent potential readings, the sensors were rinsed with

deionized water for 10 s between measurements. To affirm result dependability, the five most consistent datasets from the experimental replicates were selected for further analysis. All samples were analyzed at a temperature of 25 ± 1 °C.

2.5. Analysis of electronic nose

A Fox 4000 *E*-nose (Alpha MOS, Toulouse, France) was employed to evaluate the overall odor profiles of the samples. The Fox 4000 was equipped with 18 sensor chambers. Table 1 shows the specifications of the sensor array. TOC-grade synthetic air served as the carrier gas. For each analysis, 1 g of sample was placed in a 10 mL sealed glass vial and incubated at 50 °C for 5 min to generate headspace. The measurement phases lasted for 200 s, with a flow rate set at 200 mL/min for the transferred sample gas. Each sample was analyzed five times, and three consistent datasets were retained for further processing.

2.6. Analysis of headspace gas chromatography–mass spectrometry

Exactly 0.50 g of broad bean paste was precisely placed into a 15 mL headspace vial. Subsequently, 0.01 g of 2-methyl-3-heptanone was added as an internal standard for VOC quantification. The equipment then facilitated extraction at a stable temperature of 60 °C for 15 min, followed by a 30-min incubation time and a desorption time of 4 min. A gas chromatography-mass spectrometer (7890B-5977 A, Agilent Company, USA) equipped with a 30 m × 0.32 mm × 0.25 μm TR-5MS capillary column (J&W Company, USA) was employed for the analysis. Helium (99.999%) served as the carrier gas at a constant flow rate set at 1.2 mL/min. The temperature program was initiated at 40 °C, with the inlet temperature set at 250 °C and held for 3 min. It was then ramped up to 200 °C at a rate of 5 °C/min and maintained for 10 min, followed by a 3-min post-run, with a split ratio of 1:1. The mass spectrometer operated with a 70 eV electron impact ion source. The temperature of the ion source was set to 200 °C, and the mass scan range spanned from 30 to 550 m/z. Each sample underwent triplicate testing to ensure the stability of the results. Volatile compounds were identified by comparing their experimental mass spectra with the NIST17 mass spectral library, based on a minimum similarity degree of 80%.

Table 1
Characteristics and performance parameters of E-nose sensor array

Sensors	Performance Description	Sensors	Performance Description
P10/1	Sensitive to non-polar compounds(octane)	LY2/LG	Sensitive to strongly oxidizing gases (sulfides)
P10/2	Sensitive to non-polar flammable gases (methane, heptane)	LY2/G	Sensitive to toxic gases (methylamines)
P40/1	Sensitive to strongly oxidizing gases (methyl furfuryl disulfide)	LY2/AA	Sensitive to organic compounds (ethanol, acetone, ammonia)
PA/2	Sensitive to organic compounds (acetaldehyde,)	LY2/Gh	Sensitive to toxic gases (anilines)
P30/1	Sensitive to flammable organic compounds (ethanol)	LY2/gCTl	Sensitive to toxic gases (sulfides)
P40/2	Sensitive to strongly oxidizing gases (methanethiol)	LY2/gCT	Sensitive to flammable gases (butane, propane)
P30/2	Sensitive to organic compounds (hydrogen sulfide, ketones)	T40/2	Sensitive to strongly oxidizing gases (dimethyl disulfide)
T30/1	Sensitive to polar compounds (propanol, butane)	T40/1	Sensitive to strongly oxidizing gases (creosote)
T70/2	Sensitive to aromatic compounds (toluene and its derivatives)	TA/2	Sensitive to organic compounds (hexanol)

2.7. Calculation of relative odor activity value

The relative odor activity value (ROAV) was used to determine the significance of key VOCs in the LBBP (Bi et al., 2024). The ROAV for the most influential VOC in LBBP flavor was set at 100. The ROAVs for additional VOCs were calculated using the following formula:

$$\text{ROAV} \approx 100 \times \frac{C\%_X}{C\%stan} \times \frac{T_{stan}}{T_X}$$

Formula: C%*stan* and T*stan* represent the percentage (%) and threshold (μg/kg) of the components contributing most to the flavor in LBBP, respectively; C%*X* and T*X* denote the percentage (%) and threshold (μg/kg) of each VOC.

2.8. Data processing and statistical analysis

All data were analyzed using Microsoft Excel 2021 (Microsoft Corporation, Redmond, WA, USA). SPSS 25.0 (IBM Corporation, Armonk, NY, USA) was used to calculate the statistical significance of differences and standard deviation. Orthogonal partial least squares discrimination analysis was conducted using SIMCA 18.1 (Umetrics, Umeå, Sweden). Principal component analysis and radar plots were generated using Origin 2022 software (OriginLab Corporation, Northampton, MA, USA). Chemical structure diagrams were plotted using ChemDraw 20.0 (PerkinElmer, Waltham, MA, USA).

3. Results and discussion

3.1. Analysis of sensory evaluation

Fig. 1 and Table S2 shows the sensory scores of LBBP, with OT3 achieving the highest total sensory score, followed by IT3and OT1. Conversely, IT1 received the lowest sensory score among the LBBP samples ($P < 0.05$). OT3 was distinguished by its excellent aroma, taste, and texture despite having lower color scores. The assessment of the expert panel of the LBBP color indicated that the outdoor-treated samples exhibited a progressively darker color with each year of ripening, whereas the indoor-treated samples appeared brighter and received higher color scores. This phenomenon is hypothesized to be related to fermentation temperature: a lower fermentation temperature helps facilitate the preservation of a bright color (Zhu et al., 2022), whereas
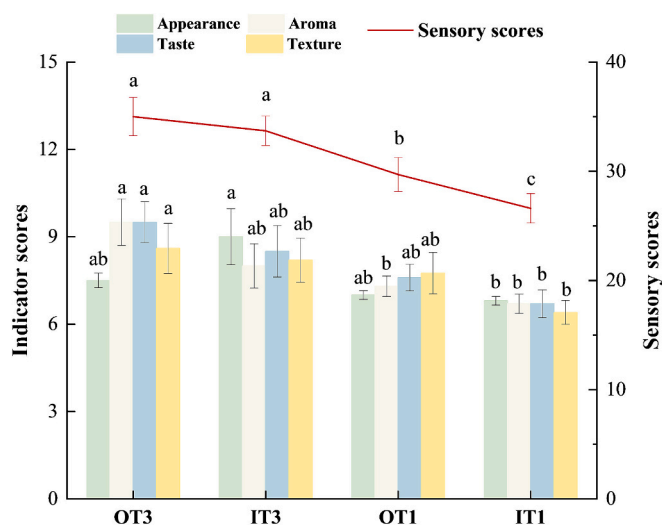

Fig. 1. Sensory socres of Linjiangsi Broad Bean after various reheating methods.
Note: OT1, and OT3 represent ripening of 1 year and 3 years in outdoor environment respectively. IT1, and IT3 were represents ripening 1 year and 3 years in indoor environment respectively.

outdoor conditions may hasten the Maillard reaction, resulting in a deeper color (Yıltırak et al., 2022). Consequently, the outdoor treatment and ripening significantly enhanced the aroma, taste, and flavor of LBBP, while the indoor treatment better preserved its original bright color.

3.2. Analysis of nutrition

Table 2 shows the fat, energy, protein, and carbohydrate contents of LBBP at different ripening times under varying environmental conditions. Ripening and environmental conditions were found to affect the nutritional content. The outdoor-treated samples showed higher amounts of nutrient consumption, including fat, energy, and protein, whereas the indoor-treated LBBP retained higher nutrient values. Additionally, nutrient decline was influenced by the duration of fermentation, with the exception of proteins, which always seem to decrease over time. This observation was more pronounced in the outdoor-treated samples ($P < 0.05$), particularly in the OT3 sample. Millena et al. (2023) reported that extending the fermentation period reduces the nutritional content. Li et al. (2022) found that during the ripening of fermented foods, enzymes, and microorganisms hydrolyze and oxidize proteins and lipids, forming numerous small-molecule flavor substances such as free amino acids, free fatty acids, aldehydes, and ketones. In outdoor environments, higher temperatures due to sun exposure—than those of indoor treatment groups—may catalyze these reactions, leading to greater nutrient degradation and increased production of volatiles. This process may explain why outdoor-treated LBBPs are more favored by trained panelists (Zhao et al., 2021).

3.3. Analysis of electronic tongue

Differences in taste characteristics were evaluated using an *E*-tongue. Fig. 2 (A) shows that all seven sensors exhibited distinct responses to the taste profiles of the four LBBP samples. OT3 showed the highest response value, indicating its richness in flavor substances. IT3 closely followed OT3 in flavor intensity, except for the SCS sensor, which displayed the lowest response. IT1 and IT3 exhibited similar taste profiles, indicating that the bean paste treated in the chamber had a more consistent flavor. The AHS and ANS sensors showed the strongest responses for OT1, whereas IT1 demonstrated the highest taste responses from the ANS, AHS, PKS, and CPS sensors.

Fig. 2 (B) shows that E-tongue detected the taste intensities of sourness, saltiness, umami, sweetness, and bitterness. Umami emerged as the most prominent taste in LBBP, especially after three years of outdoor ripening, followed by three years of indoor ripening. The intensity of these tastes, especially umami, appeared to increase with ripening time. Sour taste responses were higher after 1 year of fermentation compared to that of three years. Similarly, the duration of fermentation influenced bitterness, with the least bitterness exhibited by LBBP fermented for 1 year. This increased with longer ripening times. Wei et al. (2023) observed that bitter amino acids in fermented tofu increased gradually over the fermentation period. Research on bitter peptides and their characteristics in fermented soybean foods can enhance sensory quality and widen consumer acceptance (Jiang et al., 2023).

The PCA plot of the *E*-tongue taste differences (Fig. 2C) shows that PC1 (76.2%) and PC2 (19.3%) collectively accounted for 95.5% of the cumulative variance, reflecting the overall taste profiles of LBBP. The samples were clearly distinguishable: IT1 and OT1 clustered on the negative PC1 axis, primarily associated with the SCS sensor, whereas OT3 and IT3 clustered on the positive PC1 axis. OT3 was associated with the CPS, CTS, and PKS sensors, while IT3 correlated with the AHS, ANS, and NMS sensors.

3.4. Analysis of electronic-nose

Fig. 3 (A) shows the radar plot areas for the LBBP samples, which varied based on different ripening times and environments. The sensors P30/1 (sensitive to flammable compounds), P30/2 (sensitive to hydrogen sulfide and ketones), and PA/2 (sensitive to organic compounds such as acetaldehyde and amines) exhibited strong responses, especially to LBBP samples ripened outdoors over the years. This suggests that the ripening duration and environmental conditions influence ethanol, hydrogen sulfide, ketones, and acetaldehyde presence. Sensors P30/1 and PA/2 showed the highest response values for the OT3 and IT3 samples, indicating that ripening time significantly affects the composition of VOCs, such as ethanol, ketones, and acetaldehyde. Furthermore, the response intensity of LY2/LG, LY2/G, LY2/AA, LY2/Gh, LY2/gCTI, and LY2/gCT sensors was comparatively low, with only slight variations, suggesting reduced levels of sulfides, methylamines, anilines, butane, and propane in the LBBP samples.

Fig. 3 (B) shows the PCA results, where the first two principal components, PC1 (95.7%) and PC2 (2.90%), collectively accounted for 98.6% of the total variance, indicating that PC1 primarily captured most of the odor profile of all samples. The four LBBP samples exhibited clear differentiation, with OT3 positioned in the third quadrant, indicative of a flavor profile significantly different from that of the other samples. IT1 and IT3 appeared closer to each other, indicating a more consistent flavor profile in the indoor-fermented samples. The proximity of IT3 to OT3 suggests similarities in volatile profiles across the three ripening years. OT1, positioned in the fourth quadrant, was the furthest from the outdoor-treated samples, indicating that microbial activity and enzymatic processes during the three-year fermentation period significantly influenced compound development, thereby amplifying sensor response values (Feng et al., 2024).

3.5. Analysis of headspace gas chromatography–mass spectrometry

Table 3 shows VOCs identified in LBBP, totaling 95. These include 27 esters, 17 alkanes, 11 aldehydes, 7 olefins, 6 alcohols, 3 nitriles, 3 ketones, 3 benzenes, 3 thiophenes, 3 acids, 3 furans, 2 each of ethers, sulfides, hydrazines, and 2 other compounds. OT1, IT3, and IT1 specifically exhibited 41, 46, and 48 detected VOCs, respectively, whereas only 27 VOCs were contained in OT3.

Fig. 4A and B illustrate the number of VOCs and their concentrations in LBBP respectively, revealing significant variations in VOC profiles with ripening time and fermentation environment. Extended ripening time consistently reduced both the concentration and variety of VOCs, as evidenced by the detection of 33 esters in 1-year fermented LBBP compared to only 9 esters in 3-year fermented LBBP, and a mere 3 esters in OT3. Indoor fermentation enhanced the diversity of VOCs, particularly esters; however, as shown in Fig. 4B, despite producing a greater variety of VOCs, indoor fermentation resulted in significantly lower total VOC quantities compared to outdoor fermentation ($P < 0.001$), especially for aldehydes. Regarding alkanes, a total of 30 were detected across all LBBP samples, with IT3 exhibiting the highest abundance at 14 compounds, while all alkanes disappeared in OT3. This phenomenon may be due to incomplete fermentation at low temperatures, where flavor precursor alkanes are produced without fully developing into flavor compounds (Que et al., 2023). Although alkanes have a high
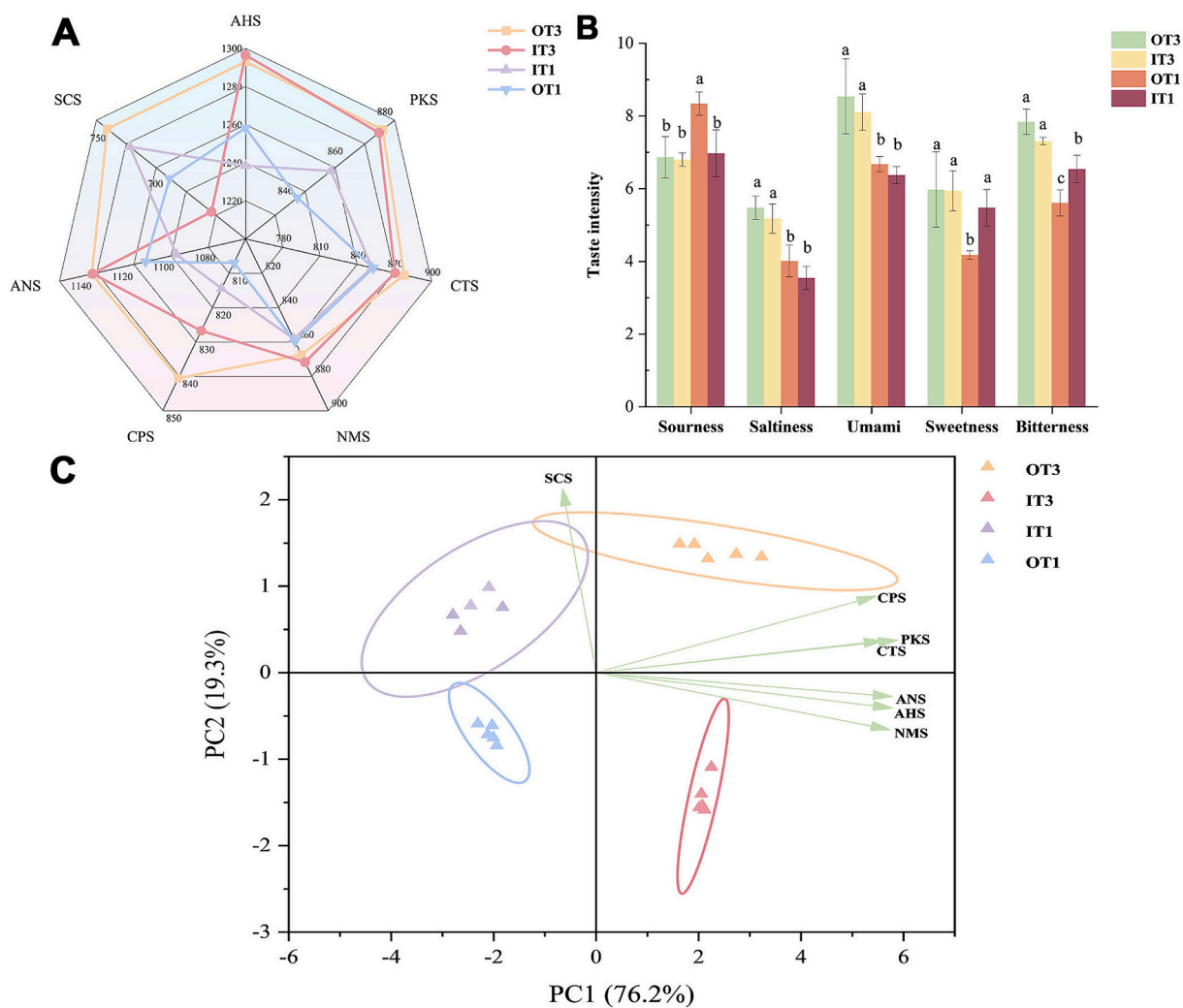
Table 2
The fat, energy, protein, and carbohydrate contents of LBBP

Nutrients	OT3	OT1	IT3	IT1
Energy(kJ/100 g)	516.00 ± 15.72^b	523.00 ± 8.49^b	576.00 ± 5.20^a	592.67 ± 14.85^a
Protein(g/100 g)	6.80 ± 0.49^d	7.40 ± 0.26^c	9.23 ± 0.07^a	8.50 ± 0.35^b
Fat(g/100 g)	1.17 ± 0.14^d	1.60 ± 0.16^{bc}	2.17 ± 0.05^{ab}	2.60 ± 0.07^a
Carbohydrate(g/100 g)	19.87 ± 0.06^c	21.80 ± 0.42^a	20.40 ± 0.10^{bc}	21.03 ± 0.35^{ab}

Fig. 2. Analysis of E-tongue in different fermentation conditions of Linjiangsi Broad Bean.
Note: (a) The radar chart of the E- tongue, (b) Taste intensity value by E-tongue (c) The PCA chart of the E-tongue.
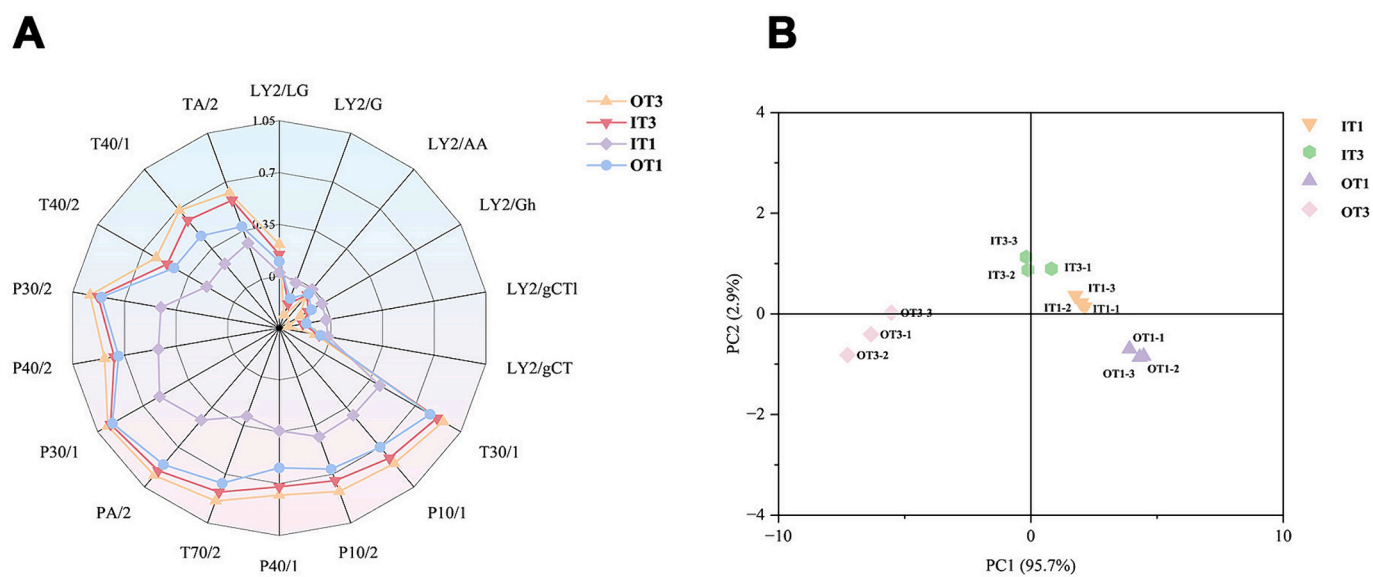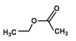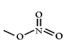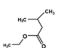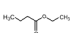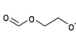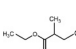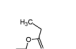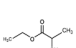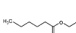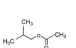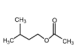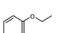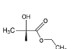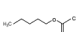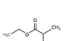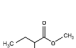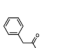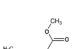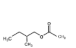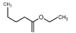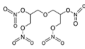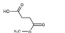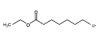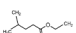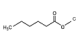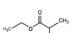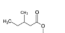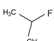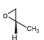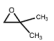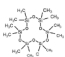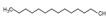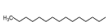

Fig. 3. Analysis of E-nose in different fermentation conditions of Linjiangsi Broad Bean.
Note: (a) The radar chart of the E- tongue, (b) The PCA chart of the E-nose.

Table 3
The volatile organic compounds of *Linjiangsi* broad bean paste

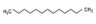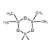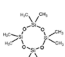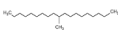| Count	Classification	Compound name	CAS#	Structural type	Formula	Molecular weight	Retention time	Relative amount (%)			
								OT3	OT1	IT3	IT1
1	Esters	Ethyl Acetate	64–17-22		C4H8O2	88.11	3.038	ND	16.57 ± 1.45	9.98 ± 0.37	ND
2		Methyl nitrate	598–58-3		CH3NO3	77.0394	2.405	1.27 ± 0.23[b]	0.86 ± 0.12[c]	0.06 ± 0.01[d]	4.52 ± 0.30[a]
3		Ethyl isovalerate	108–64-5		C7H14O2	130.18	8.624	0.10 ± 0.53[c]	0.67 ± 0.14[b]	0.85 ± 0.11[a]	0.15 ± 0.01[c]
4		Ethyl butanoate	105–54-4		C6H12O2	116.16	5.456	ND	1.06 ± 0.14	0.53 ± 0.03	ND
5		1,2-Diformyloxyethane	629–15-2		C4H6O4	118.09	20.526	ND	0.95 ± 0.11	ND	ND
6		Ethyl 2-methylbutanoate	7452–79-1		C7H14O2	130.18	8.449	ND	0.22 ± 0.04	0.62 ± 0.0	ND
7		n-Ethyl propanoate	105–37-3		C5H10O2	102.13	4.351	ND	0.17 ± 0.02	0.34 ± 0.03	ND
8		Ethyl isobutyrate	97–62-1		C6H12O2	116.16	4.981	ND	ND	0.48 ± 2.82	ND
9		Ethyl hexanoate	123–66-0		C8H16O2	144.21	14.765	ND	ND	0.29 ± 0.03	ND
10		Isobutyl acetate	110–19-0		C6H12O2	116.158	5.881	ND	0.2 ± 0.04	0.06 ± 0.01	ND
11		Isoamyl acetate	123–92-2		C7H14O2	130.185	5.881	ND	0.2 ± 0.04	0.06 ± 0.01	ND
12		Ethyl crotonate	6776-19-8		C6H10O2	114.14	7.699	ND	ND	0.23 ± 0.06	ND
13		(−)-Ethyl L-lactate	687–47-8		C5H10O3	118.13	7.044	ND	0.23 ± 0.04	ND	ND
14		Pentyl acetate	628–63-7		C7H14O2	130.18	9.416	ND	ND	ND	0.17 ± 0.03
15		Ethyl lactate	97–64-3		C5H10O3	118.13	6.661	ND	ND	0.03 ± 0.01	ND
16		Methyl 2-methylbutyrate	868–57-5		C6H12O2	116.16	5.852	ND	ND	0.14 ± 0.01	ND
17		Ethyl phenylacetate	101–97-3		C10H12O2	164.2	25.604	ND	ND	0.04 ± 0.01	0.09 ± 0.01
18		2,4-Hexadienoic acid, methyl ester	1515-80-6		C7H10O2	126.15	16.278	0.12 ± 0.06	ND	ND	ND
19		2-Methylbutylacetate	624–41–9		C7H14O2	130.18	9.529	ND	ND	0.12 ± 0.05	ND
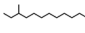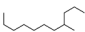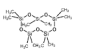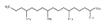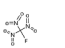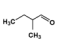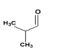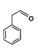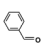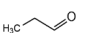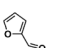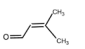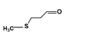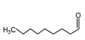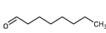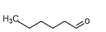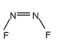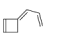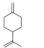
6

Table 3 (*continued*)

Count	Classification	Compound name	CAS#	Structural type	Formula	Molecular weight	Retention time	Relative amount (%)			
								OT3	OT1	IT3	IT1
20		Ethyl valerate	539–82-2		C7H14O2	130.19	10.634	ND	0.02 ± 0.01	0.08 ± 0.01	ND
21		3,3'-Oxybis(1,2-propanediol) tetranitrate	20,600–96-8		C6H10N4O13	346.16	3.993	ND	0.07 ± 0.01	ND	ND
22		4-Methoxy-4-oxobutanoic acid	3878-55-5		C5H8O4	C5H8O4	10.738	ND	ND	ND	0.06 ± 0.01
23		Ethyl caprylate	106-32-1		C10H20O2	172.26	20.506	ND	ND	0.06 ± 0.01	ND
24		Ethyl 4-methyl valerate	25,415–67-2		C8H16O2	144.2114	13.344	ND	0.02 ± 0.01	0.03 ± 0.01	ND
25		Methyl hexoate	106–70-7		C7H14O2	130.18	11.338	ND	ND	0.04 ± 0.01	ND
26		Ethyl lactate	97–64-3		C5H10O3	118.13	6.661	ND	ND	0.03 ± 0.01	ND
27		Ethyl 3-methylpentanoate	5870-68-8		C8H16O2	144.21	15.378	ND	0.02 ± 0.01	ND	ND
28	Alkanes	2-Fluoropropane	420–26-8		C3H7F	62.09	2.280	ND	8.36 ± 0.77	ND	ND
29		(*S*)- (−)-Propylene oxide	16,088–62-3		C3H6O	58.08	2.292	ND	ND	ND	5.91 ± 0.38
30		Isobutylene Oxide	558–30-5		C4H8O	72.11	2.655	ND	1.83 ± 0.15[a]	0.52 ± 0.08[b]	0.25 ± 0.04[c]
31		Dodecamethylcyclohexasiloxane	540–97-6		C12H36O6Si6	444.9236	30.677	ND	0.38 ± 0.05[b]	0.46 ± 0.04[b]	1.12 ± 0.05[a]
32		Tetradecane	629–59-4		C14H30	198.39	34.83	ND	0.11 ± 0.02[b]	0.12 ± 0.02[b]	0.23 ± 0.05[a]
33		Pentadecane	629–62-9		C15H32	212.4146	39.307	ND	0.03 ± 0.01	ND	0.35 ± 0.04
34		Tetradecamethyl Cycloheptasiloxane	107–50-6		C14H42O7Si7	519.08	34.942	ND	ND	ND	0.28 ± 0.04
35		Tridecane	629–50-5		C13H28	184.36	30.436	ND	0.06 ± 0.02[b]	0.05 ± 0.01[b]	0.17 ± 0.03[a]
36		Hexamethylcyclotrisiloxane	541–05-9		C6H18O3Si3	222.46	7.074	ND	ND	0.13 ± 0.02	0.14 ± 0.02
37		Octamethylcyclotetrasiloxane	556–67-2		C8H24O4Si4	296.62	14.169	ND	ND	0.1 ± 0.01	0.09 ± 0.01
38		10-Methylnonadecane	56,862–62-5		C20H42	282.54748	30.823	ND	ND	0.08 ± 0.01	0.09 ± 0.01
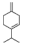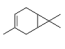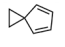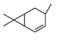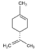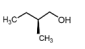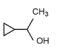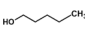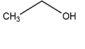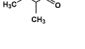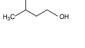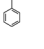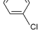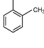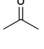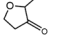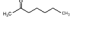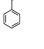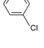
Table 3 (*continued*)

Count	Classification	Compound name	CAS#	Structural type	Formula	Molecular weight	Retention time	Relative amount (%)			
								OT3	OT1	IT3	IT1
39		3-Methyltridecane	6418-41-3		C14H30	198.388	33.041	ND	ND	0.03 ± 0.01	0.09 ± 0.01
40		Hexadecane	544–76-3		C16H34	226.44	39.252	ND	ND	ND	0.12 ± 0.02
41		4-Methylundecane	2980-69-0		C12H26	170.33	30.761	ND	ND	ND	0.07 ± 0.01
42		Decamethylcyclopentasiloxane	541–02-6		C10H30O5Si5	370.77	20.685	ND	ND	ND	0.04 ± 0.01
43		2,6,10,14-Tetramethylheptadecane	18,344–37-1		C21H44	296.57	33.341	ND	ND	0.04 ± 0.01	ND
44		Fluorotrinitro methane	1840-42-2		CFN3O6	169.03	3.734	ND	ND	0.02 ± 0.01	ND
45	Aldehydes	2-Methylbutanal	96–17-3		C5H10O	86.13	3.601	29.13 ± 1.81[a]	11.36 ± 1.00[c]	3.32 ± 0.09[d]	14.89 ± 0.33[b]
46		Isobutyral dehyde	78–84-2		C4H8O	77.0394	2.646	4.24 ± 0.28[a]	ND	1.03 ± 0.04[b]	0.84 ± 0.06[b]
47		Benzeneacet aldehyde	122–78-1		C8H8O	120.15	17.500	7.87 ± 0.09[a]	0.37 ± 0.10[c]	0.16 ± 0.03[c]	2.3 ± 0.10[b]
48		Benzaldehyde	100–52-7		C7H6O	106.12	13.373	1.23 ± 0.22[a]	0.36 ± 0.08[b]	0.27 ± 0.03[b]	1.3 ± 0.11[a]
49		Propionaldehyde	123–38-6		C3H6O	58.08	2.375	1.76 ± 0.10	ND	ND	ND
50		Furfural	98–01-1		C5H4O2	86.08	7.741	0.23 ± 0.11[a]	0.04 ± 0.01[b]	0.28 ± 0.03[a]	0.08 ± 0.01[b]
51		3-Methyl-2-butenal	107–86-8		C5H8O	84.12	6.198	ND	0.14 ± 0.04	ND	0.23 ± 0.03
52		Methional	3268-49-3		C4H8OS	104.17	10.809	0.11 ± 0.06[a]	0.07 ± 0.01[b]	ND	0.19 ± 0.01[a]
53		Nonanal	124–19-6		C9H18O	142.24	20.764	10.51 ± 0.15	0.03 ± 0.01	ND	0.09 ± 0.01
54		Octanal	124–13-0		C8H16O	128.21	15.144	5.91 ± 0.12	ND	ND	0.12 ± 0.03
55		Hexanal	66–25-1		C6H12O	100.16	6.152	3.45 ± 0.06	ND	ND	0.12 ± 0.03
56	Alkenes	(Z)-Difluorodiazene	13,812–43-6		F2N2	66.01	2.267	ND	ND	5.83 ± 0.22	ND
57		(3E)-3-prop-2-enylidenecyclobutene	52,097–85-5		C7H8	92.14	5.669	0.62 ± 0.12	ND	ND	ND
58		Pseudo-limonene	499–97-8		C10H16	136.23	20.526	0.44 ± 0.10	ND	ND	ND
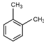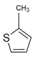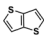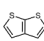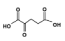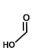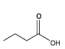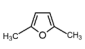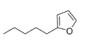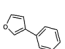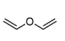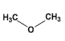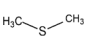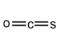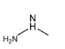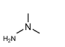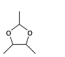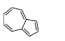
Table 3 (*continued*)

Count	Classification	Compound name	CAS#	Structural type	Formula	Molecular weight	Retention time	Relative amount (%)			
								OT3	OT1	IT3	IT1
59		Beta-terpinene	99–84-3		C10H16	136.23	17.454	ND	ND	0.17 ± 0.02	ND
60		3-Carene	13,466–78-9		C10H16	136.23	17.742	0.15 ± 0.04	ND	ND	ND
61		Spiro [2,4] hepta-4,6-diene	765–46-8		C7H8	92.14	5.444	ND	ND	0.11 ± 0.02	ND
62		(1S,3R) -(Z)-4-carene	5208-49-1		C10H16	136.23	17.437	ND	ND	ND	0.11 ± 0.01
63		D-Limonene	5989-27-5		C10H16	136.23	16.808	0.09 ± 0.02	ND	ND	ND
64	Alcohols	(*S*)-(−)-2-Methylbutanol	1565-80-6		C5H12O	88.148	5.014	ND	6.68 ± 0.34	ND	7.92 ± 0.44
65		1-Cyclopropylethanol	765–42-4		C5H10O	86.13	3.472	7.04 ± 0.53[a]	1.97 ± 0.23[c]	ND	4.28 ± 0.14[b]
66		1-Pentanol	71–41-0		C5H12O	88.15	4.923	ND	2.89 ± 0.29[b]	2.17 ± 0.07[c]	4.21 ± 0.31[a]
67		Ethanol	64–17-5		C2H6O	46.068	2.263	0.74 ± 0.07[c]	4.1 ± 0.24[a]	0.03 ± 0.08[d]	1.43 ± 0.06[b]
68		2-Methylbutan-1-ol	137–32-6		C5H12O	88.15	4.893	ND	ND	4.58 ± 0.40	ND
69		3-Methyl-1-butanol	123–51-3		C5H12O	88.15	4.943	0.95 ± 0.10	ND	ND	ND
70	Nitriles	Ethylbenzene	100–41-4		C8H10	106.17	9.175	1.05 ± 0.14	ND	ND	0.07 ± 0.01
71		Chlorobenzene	108–90-7		C6H5Cl	112.56	8.216	0.60 ± 0.15	ND	ND	ND
72		o-Xylene	95–47-6		C8H10	106.17	8.583	ND	ND	0.23 ± 0.06	ND
73	Ketones	Acetone	67–64-1		C3H6O	58.08	2.355	ND	4.08 ± 0.15	ND	ND
74		2-Methyltetrahydrofuran-3-one	3188-00-9		C5H8O2	100.12	6.886	ND	0.07 ± 0.01	ND	0.06 ± 0.01
75		2-Heptanone	110–43-0		C7H14O	114.19	9.617	ND	ND	0.07 ± 0.01	ND
76	Benzene	Ethylbenzene	100–41-4		C8H10	106.17	9.175	1.05 ± 0.14	ND	ND	0.07 ± 0.01
77		Chlorobenzene	108–90-7		C6H5Cl	112.56	8.216	0.60 ± 0.15	ND	ND	ND

Table 3 (*continued*)

Count	Classification	Compound name	CAS#	Structural type	Formula	Molecular weight	Retention time	Relative amount (%)			
								OT3	OT1	IT3	IT1
78		o-Xylene	95–47-6		C8H10	106.17	8.583	ND	ND	0.23 ± 0.06	ND
79	Thiophene	Methyl thiol	554–14-3		C5H6S	98.17	5.760	0.78 ± 0.11	ND	ND	ND
80		Thieno[3,2-b] thiophene	251–41-2		C6H4S2	140.23	25.604	0.51 ± 0.11^a	0.08 ± 0.01^b	0.06 ± 0.01^b	ND
81		Thieno[2,3-b] thiophene	250–84-0		C6H4S2	140.23	24.528	ND	ND	ND	0.21 ± 0.04
82	Acids	2-Ketoglutaric acid	328–50-7		C5H6O5	146.1	11.380	0.07 ± 0.01^b	ND	0.02 ± 0.01^c	0.3 ± 0.03^a
83		Formic acid	64–18-6		CH2O2	46.03	2.546	ND	1.06 ± 0.13	ND	0.13 ± 0.02
84		3-Methylbutanoic acid	503–74-2		C5H10O2	102.13	8.270	ND	0.02 ± 0.01	ND	ND
85	Furans	2,5-Dimethylfuran	625–86-5		C6H8O	96.13	4.222	1.01 ± 0.12	0.06 ± 0.01^c	ND	0.43 ± 0.05^b
86		2-Amylfuran	3777-69-3		C9H14O	138.21	14.869	5.35 ± 0.05	ND	ND	ND
87		3-Phenylfuran	13,679–41–9		C10H8O	144.17	25.566	ND	ND	ND	0.05 ± 0.01
88	Ethers	Vinyl ether	109–93-3		C4H6O	70.09	2.634	ND	ND	ND	0.44 ± 0.08
89		Dimethyl ether	115–10-6		C2H6O	46.07	2.763	ND	0.15 ± 0.06	ND	0.12 ± 0.02
90	Sulfurs	Dimethyl sulfide	75–18-3		C2H6S	62.13	2.496	8.16 ± 0.28	ND	ND	ND
91		Carbonyl sulfide	463–58-1		COS	60.07	2.934	ND	ND	0.39 ± 0.03	ND
92	Hydrazines	Methylhydrazine	60–34-4		CH6N2	46.07	3.284	ND	0.78 ± 0.09	ND	ND
93		1,1-Dimethylhydrazine	57–14-7		C2H8N2	60.1	2.913	ND	ND	0.26 ± 0.02	ND
94	Others	Acetaldehyde 2,3-butane diol acetal	3299-32-9		C6H12O2	116.1583	4.710	0.26 ± 0.03	ND	ND	ND
95		Azulene	275–51-4		C10H8	128.17	21.089	ND	ND	ND	0.04 ± 0.01

ND means not detected, a, b, c Means with different letters within a row differ significantly ($P < 0.05$). ±: standard deviation. OT3 means Outdoor-treated 3 year, OT1 means Outdoor-treated 1 year, IT3 means Indoor-treated 3 year, IT means: Indoor -treated 1 year; $n = 3$.
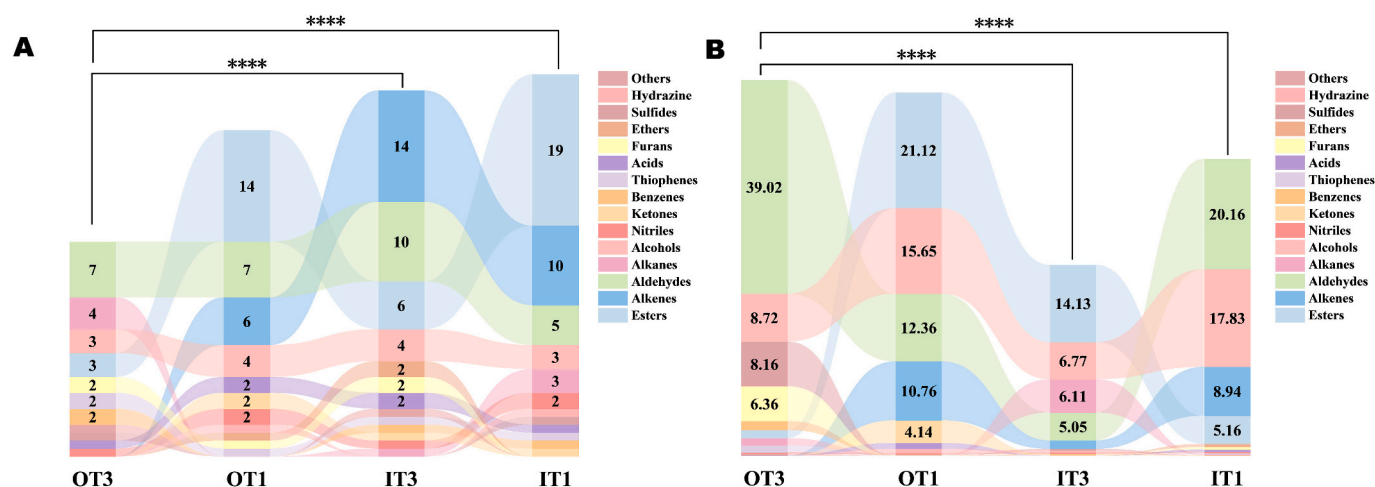
Fig. 4. Analysis of volatile organic compounds of Linjiangsi Broad Bean in different fermentation conditions.
Note: (A) The number of VOCs of Linjiangsi Broad Bean in different fermentation conditions, (B) The concentrtion of VOCs of Linjiangsi Broad Bean in different fermentation conditions.

perception threshold and low flavor contribution, they serve as precursors for heterocyclic compounds (Ye et al., 2022). During outdoor fermentation, sunlight-induced temperature increase is hypothesized to promote the conversion of alkanes into furan compounds, thereby significantly elevating the content of 2-pentyl furan in OT3 (Wu et al., 2019).

Table 4
The relative odor activity value of volatile organic compounds

Classification	Compounds	Flavor description[a]	Odor Threshold value(μg/kg) [b]	ROAV			
				OT3	OT1	IT3	IT1
Aldehydes	2-Methylbutanal	Fruity, nuts, coffee, caramel	0.80	100.00 ± 0.00	100.00 ± 0.00	100.00 ± 0.00	100.00 ± 0.00
	Octanal	Fruity	0.70	23.15 ± 1.04	ND	ND	0.89 ± 0.08
	Isobutyr aldehyde	Caramel, cocoa and Sweet	1.50	7.77 ± 0.49[b]	ND	11.09 ± 0.68[a]	3.01 ± 0.35[c]
	Hexanal	Green, fresh grass	4.50	6.89 ± 0.47	ND	ND	0.14 ± 0.08
	Benzeneacet aldehyde	Honey, sweet	4.00	5.40 ± 0.36[a]	0.65 ± 0.14[c]	0.64 ± 0.21[c]	3.09 ± 0.15[b]
	Nonanal	Fat, citrus	7.00	4.12 ± 0.63[a]	0.03 ± 0.01[b]	ND	0.07 ± 0.03[b]
	Methional	Onion, meat	0.20	1.57 ± 0.30[b]	2.29 ± 1.27[b]	ND	5.16 ± 0.39[c]
	Propanal	Grass	15.10	0.32 ± 0.11	ND	ND	ND
	3-Methyl-2-butenal	Pill	29.14	ND	0.03 ± 0.01	ND	0.04 ± 0.01
	Benzaldehyde	Almond, fruity	350.00	0.01 ± 0.01	0.01 ± 0.02	0.01 ± 0.00	0.02 ± 0.01
Esters	Ethyl 2-methylbutanoate	Green, flower, fruity	0.10	ND	15.49 ± 1.22	16.00 ± 1.16	ND
	Methyl 2-methylbutyrate	Fruity	0.06	ND	ND	17.82 ± 1.10	ND
	Ethyl 4-methyl valerate	Pineapple	0.10	ND	1.48 ± 0.15	5.51 ± 0.21	ND
	n-Ethyl propanoate	Pineapple	1.84	ND	0.66 ± 0.12	2.97 ± 0.47	ND
	Ethyl isovalerate	Apple	6.89	0.04 ± 0.02[c]	0.69 ± 0.13[b]	1.99 ± 0.08[a]	0.11 ± 0.02[c]
	Ethyl phenylacetate	Honey	0.47	ND	ND	1.21 ± 0.10	1.03 ± 0.27
	2-Methylbutylacetate	Sweet, fruity	1.10	ND	ND	1.69 ± 0.09	ND
	Pentyl acetate	Sweet, fruity, ripe pear	1.00	ND	ND	ND	0.91 ± 0.14
	Ethyl acetate	Fruity, sweet, grape, cherry	5.00	ND	0.16 ± 0.09	0.22 ± 0.07	ND
	Ethyl caprylate	Sweet, Pineapple	5.00	ND	ND	0.20 ± 0.06	ND
	Isoamyl acetate	Sweet, fruity	93.90	ND	0.01 ± 0.06	0.03 ± 0.01	ND
	Ethyl butanoate	Fruity, flower	81.15	ND	0.09 ± 0.03	0.11 ± 0.02	ND
	Methyl hexoate	Sweet, fruity	70.00	ND	ND	0.01 ± 0.01	ND
	Ethyl isobutyrate	Osmanthus, fruity	57.47	ND	ND	0.13 ± 0.17	ND
	Ethyl valerate	Fruity, floral, sweet	26.68	ND	ND	0.05 ± 0.05	ND
	Ethyl L (−)-lactate	Winey	14.00	ND	ND	ND	0.06 ± 0.03
Furans	2-Pentyl furan	Nutty, caramel	6.00	2.45 ± 0.24	ND	ND	ND
	3-Phenyl furan	Caramel	5.90	ND	ND	ND	0.04 ± 0.02
Benzene	Ether	Sweet	8.80	0.33 ± 0.08	ND	ND	0.04 ± 0.05
	o-Xylene	Candy	450.20	ND	ND	0.01 ± 0.02	ND
	1-Pentanol	Fat, sweet, bread, grain	400.00	ND	0.01 ± 0.05	0.01 ± 0.01	0.01 ± 0.01
Others	Pentadecane	Grass, flower	3.00	ND	0.08 ± 0.03	ND	0.62 ± 0.14
	Dimethyl sulfide	Onions, corn, roast	0.02	11.21 ± 0.63	ND	ND	ND
	Methyl thiol	Flower, grass	34.00	0.06 ± 0.07	ND	ND	ND
	2-Heptanone	Peer, apple	140.00	ND	ND	0.01 ± 0.02	ND

[a] : The flavor descriptions are obtained from the technology of food flavoring (Sun, 2017) and http://www.odour.org.uk
[b] : The aroma threshold of flavor compounds is mainly derived from the Technology of Food Flavoring (Sun, 2017), ND means not detected, a, b, c Means with different letters within a row differ significantly (P < 0.05). ±: standard deviation. OT3: Outdoor-treated 3 year, OT1: Outdoor-treated 1 year, IT3: Indoor-treated 3 year, IT1: Indoor -treated 1 year. n = 3

### 3.6. Analysis of relative odor activity value

In addition to content relevance, the VOC threshold values also warrant consideration, as they collectively determine their authentic contribution to the overall aroma characteristics. Consequently, the ROAV was used to assess the influence of VOCs on the comprehensive aroma profile, which can evaluate the real contribution of characteristic flavor compounds (Bi et al., 2024). The compounds with ROAV ≥ 1 significantly influence the flavor profile of LBBP, while those with ROAV between 0.1 and 1 indicate a moderate influence on its overall aroma. Table 4 lists the sensory descriptions and threshold values of these VOCs in LBBP.

Among the identified VOCs, 2-methylbutanal stands out because of its high LBBP content and low odor threshold (0.8 μg/kg). Consequently, we assigned the ROAV *stan* at 100 for 2-methylbutanal. Overall, 16 VOCs with ROAV ≥ 1 were identified in the LBBP. These compounds include 8 esters: ethyl isovalerate, ethyl 2-methylbutanoate, n-ethyl propanoate, methyl 2-methylbutyrate, ethyl phenylacetate, 2-methylbutylacetate, and ethyl 4-methyl valerate; 7 aldehydes: 2-methylbutanal, isobutyraldehyde, benzeneacetaldehyde, methional, nonanal, octanal, and hexanal; and 2 heterocyclic compounds: 2-pentyl furan and dimethyl sulfide. Fig. 5 shows the ROAV values and hierarchical cluster analysis of LBBP. OT3 and IT3 clustered together on the left side. OT3 exhibited the highest concentrations of aldehydes and heterocyclic compounds. This observation suggests a correlation with increased fermentation temperatures induced by sunlight exposure, which alters the microbial fermentation environment. Additionally, elevated fermentation temperatures accelerate the Maillard reaction rate, thereby further enhancing aldehyde contribution. During the Maillard reaction, compounds formed include furfural, benzaldehyde, and hexanal (Luo et al., 2021). The influence of ripening time and fermentation environment on VOCs in LBBP was notable, especially concerning

aldehydes. Aldehyde levels from 3 years of outdoor fermentation specifically increased by 24.80% compared to those from 1 year. Regarding indoor-treated LBBP, IT3 exhibited the highest ester abundance. Previous research on traditional soy sauce shows that alcohols and esters are the dominant compounds (Devanthi & Gkatzionis, 2019). Zhao et al. (2021) observed significant increases in acidity, amino nitrogen, alcohols, and esters owing to the absence of sunlight exposure or air. Consequently, the fermentation environment and ripening time play pivotal roles in shaping the VOC profile of LBBP, thereby resulting in distinct characteristic flavor profiles.

3.7. Analysis of key volatile flavor compounds from the Linjiangsi broad bean paste

Aldehydes—characterized by their low odor threshold in foods—contribute significantly to the distinctive flavor profile of fermented condiments (Lin, Fu, et al., 2022). They impart pleasing flavors reminiscent of caramel, nuts, green notes, and roasts. Additionally, aldehydes can participate in linkage or condensation reactions with alcohols, methanethiols, and ammonia, thereby enriching the bean paste with a more complex aroma profile (Zhang et al., 2023).

Branched-chain aldehydes are often generally appreciated for their sweet or fruity taste, such as 2-methylbutyraldehyde, which evokes aromas of fruits, nuts, coffee, and caramel (Smit et al., 2009). 2-methylbutanal—a key odorant in fermented products such as soy sauce and cheese—is primarily produced by microorganisms (Tian et al., 2023). Its synthesis is largely attributed to the Ehrlich and amino acid biosynthesis pathways involving branched-chain amino acids, including leucine, valine, and isoleucine (Steinhaus & Schieberle, 2007).

Nonanal, octanal, and hexanal were identified to have significant roles in OT3 (ROAV >1), especially octanal. In contrast, indoor-treated 1-year LBPP was found to have a modest contribution to LBBP (ROAV <
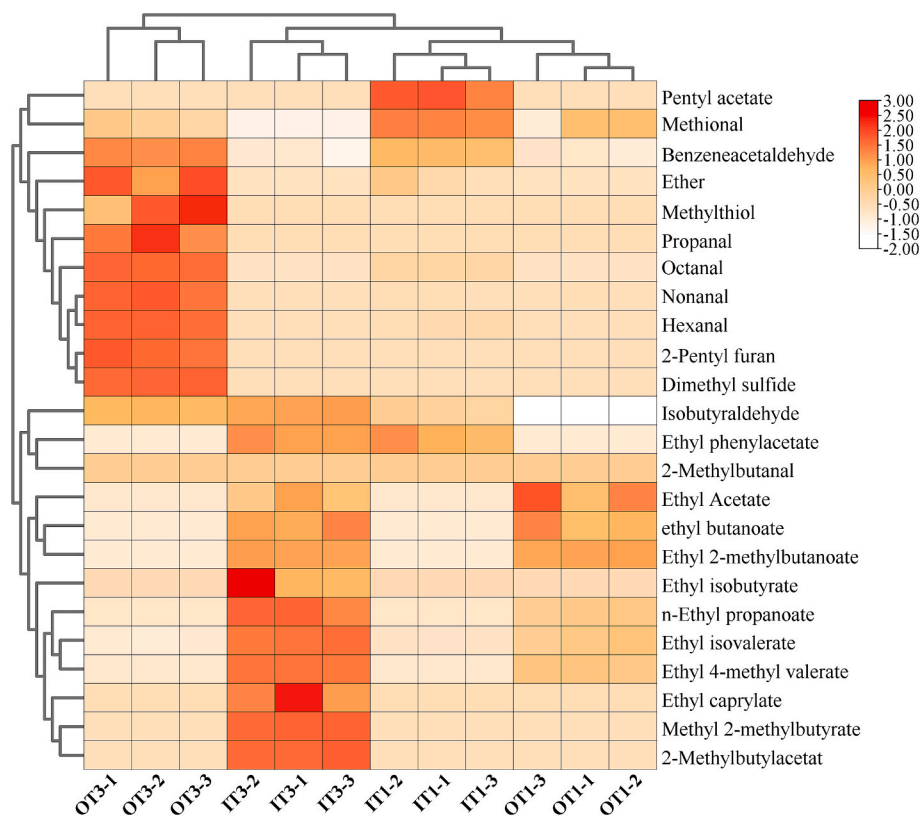

Fig. 5. The cluster heat map of ROAV of Linjiangsi Broad Bean in different fermentation conditions.
Note: OT1, and OT3 represent ripening of 1 year and 3 years in outdoor environment; IT1, and IT3 were represents ripening 1 year and 3 years in indoor environment.

1), whereas no contribution to OT1 and IT3 was observed. Octanal, with a low threshold (0.7 µg/kg), imparts a pronounced fruity aroma and is formed through the autoxidation degradation of oleic acid (C18:1) (Olivares et al., 2011). Hexanal is a quintessential compound known for its grassy and fresh aroma and has been identified as a significant contributor to fermented bean condiments (Lv et al., 2011). Similar to octanal, hexanal plays a vital role in OT3 and contributes modestly to IT1. However, it does not contribute to OT1 and IT3. Hexanal is a characteristic aldehyde resulting from the oxidative degradation of linoleic acid (C18:2) and is typically used as an indicator for lipid oxidation (Azarbad & Jeleń, 2014). The significant variation in the contribution of hexanal could be attributed to continuous sunlight exposure in outdoor fermentation environments, which accelerates the oxidation of linoleic acid. Similar to hexanal, nonanal is also formed as a lipid oxidation product through the autoxidation of linoleic acid, imparting a fatty citrus aroma to LBBP. This compound was identified as a key contributor to the aroma of LBBP, specifically in OT3 samples. During fermentation, *Aspergillus flavus*, a predominant fungus, emerged as a major pathogen that causes safety concerns for fermented foods. However, previous research indicates that octanal and nonanal can inhibit the growth of *Aspergillus flavus*, thereby enhancing the safety of the fermentation process (Zhang et al., 2017). Octanal and nonanal are commonly identified in fermented foods such as sufu, broad bean paste, and soy sauce (Diez-Simon et al., 2020; Zhao et al., 2021). Tang et al. (2019) investigated the fermentation process of broad bean paste. Besides visible light and radiation, ultraviolet (UV) exposure also contributes to the formation of hexanal, octanal, and nonanal. UV light interacts with the aqueous phase in beans, leading to the production of carbon oxide compounds with aldehyde-like flavor characteristics.

Isobutyraldehyde imparts caramel, cocoa, and sweet aromas formed through the Strecker reaction during alanine degradation. It can undergo further oxidation to carboxylic acids or reduction, forming alcohols (Sanderson & Grahamm, 1973). Isobutyraldehyde plays a significant role in outdoor-treated and indoor-treated samples, with 3 years of fermentation treatment increasing its flavor contribution. In contrast, the contribution of methional is strongly influenced by ripening time, with the highest levels observed in IT1, followed by OT1. However, its concentrations decreased across all three-year fermentation samples, particularly in the indoor-fermented LBBP. Propanal imparts grassy notes and octanal in LBBP, contributing exclusively to the outdoor-treated LBBP after 3 years.

Esters play a crucial role as primary flavor compounds in soybean paste owing to their low odor threshold and high volatility, contributing sweet and fruity notes while effectively masking the bitter and pungent aromas of fatty acids (Li et al., 2017; Yu et al., 2022). Esters can be formed through two main pathways: enzymatic reactions catalyzed by microorganisms—such as yeasts, molds, and bacteria—and non-enzymatic esterification of organic acids with alcohols (Que et al., 2023). Most esters were detected in the indoor-fermented LBBP, whereas the outdoor-treated samples showed only two key compounds. Seven VOCs significantly contributed to the flavor profile of IT3, including ethyl isovalerate, ethyl 2-methylbutanoate, n-ethyl propanoate, methyl 2-methylbutyrate, ethyl phenylacetate, 2-methylbutylacetate, and ethyl 4-methyl valerate. Methyl 2-methylbutyrate stands out among them as the most abundant ester compound, imparting a fruity aroma to LBBP owing to its remarkably low threshold (0.06 µg/kg).

Barba et al. (2018) explored the enhancement of sweetness in fruit juices by 2-Methylbutylaceta. Additionally, previous research found that the concentration of ester aromatic compounds, such as methyl 2-methylbutyrate, decreased significantly after 15 min of UV irradiation (Manzocco et al., 2016). This reduction may be attributed to the absence of esters in LBBP fermented outdoors for 3 years. 2-Methylbutylacetate, akin to methyl 2-methylbutyrate, was detected exclusively in the indoor-treated three-year LBBP (IT3) sample, which acts as a significant flavor compound (ROAV >1). Furthermore, n-ethyl propanoate and ethyl isovalerate have emerged as crucial flavor contributors to IT3, which

imparts pineapple and apple notes. Ethyl isovalerate—biologically synthesized from the branched-chain amino acid L-leucine—contrasts with n-ethyl propanoate, which results from the esterification of propionic acid (Lin, Zeng, et al., 2022). These two compounds acted as modest contributors to OT1 (ROAV <1). Similar to ethyl 2-methylbutanoate, ethyl 4-methyl valerate was detected only in OT1 and IT3, and it can be a key contributor to the fruity aroma, though it contributes more to IT3. Similarly, Ethyl 2-methylbutanoate and ethyl 4-methyl valerate were detected only in OT1 and IT3. Whereas both contribute to fruity aromas, ethyl 4-methyl valerate has a greater impact on IT3. Ethyl acetate, found exclusively in OT1 and IT3, contributed modestly to flavor because of its low content (ROAV <1). Finally, Ethyl phenylacetate, a marker compound, distinguished indoor-fermented LBBP from other processed methods.

Aldehydes and esters play significant roles in shaping the characteristic LBBP flavor, and their production varies greatly based on the fermentation environment and ripening time. Aldehydes arise primarily from Maillard reactions, lipid degradation, and Strecker pathways, which are necessary for elevated temperatures, radiation, or UV exposure for synthesis. Conversely, at lower temperatures, esters are predominantly synthesized by microorganisms such as yeasts, molds, and bacteria. Higher temperatures disrupt microbial homeostasis, resulting in the absence of esters in outdoor-fermented LBBP. Overall, aldehydes and esters significantly differentiate the outdoor and indoor LBBP flavor profiles. Aldehydes frequently contribute to nutty, coffee, and caramel aromas, whereas esters impart fruity notes. These differences become more pronounced with extended ripening times.

Similar to the production mechanism of most aldehydes, furans are produced through the Maillard reaction or lipid degradation. Additionally, alcohols and phenols can serve as precursors for furan formation at high fermentation temperatures (Li et al., 2024)0.2-Pentyl furan, a key compound, contributes specifically to the nutty and caramel aromas in OT3. Sulfur-containing compounds play a vital role in LBBP as even minute traces of them can significantly contribute to its flavor. These compounds originating from sulfur-containing amino acids, such as methionine, undergo Strecker degradation to generate thiols, which subsequently oxidize into sulfur compounds (Starowicz & Zieliński, 2019). Dimethyl sulfide, detected only in OT3, imparts onion, corn, and roasted notes, significantly influencing the characteristic flavor of outdoor-fermented LBBP. Given their uniqueness, 2-pentyl furan and dimethyl sulfide serve as characteristic flavor markers for outdoor-fermented LBBP. Finally, ethers, which contribute to a sweet aroma and mitigate salty and bitter tastes, were modestly present solely in OT3.

3.8. Analysis of multivariate statistic

Orthogonal partial least squares discriminant analysis (OPLS-DA) was employed to further investigate the aroma distinctions of LBBP across different ripening times and fermentation environments using ROAV contribution values as input data. The cumulative statistical value of the model $R^2X = 0.953$, model explanation rate parameter $R^2Y = 0.987$, and predictive ability parameter $Q^2 = 0.978$ all exceeded 0.5, demonstrating the robust explanatory power of the model in analyzing aroma differences in LBBP.

Fig. 6 (A) shows a scatter plot of the scores, revealing distinct differences among various samples. Samples fermented for one year are positioned in the upper half of the plot, while three-year fermented samples appear in the lower half. This indicates that the LBBP flavor profile changes with different fermentation periods. Fig. 6 (B) shows the internal relationships within the LBBP samples. Samples fermented for one year showed closer proximity, but after three years of fermentation, OT3 was located in the upper right quadrant, whereas IT3 was in the lower left quadrant. This indicated that minimal differences were affected by different fermentation environments on flavor during the initial fermentation stages. However, after three years, a significant distinctive flavor profile emerged between indoor and outdoor
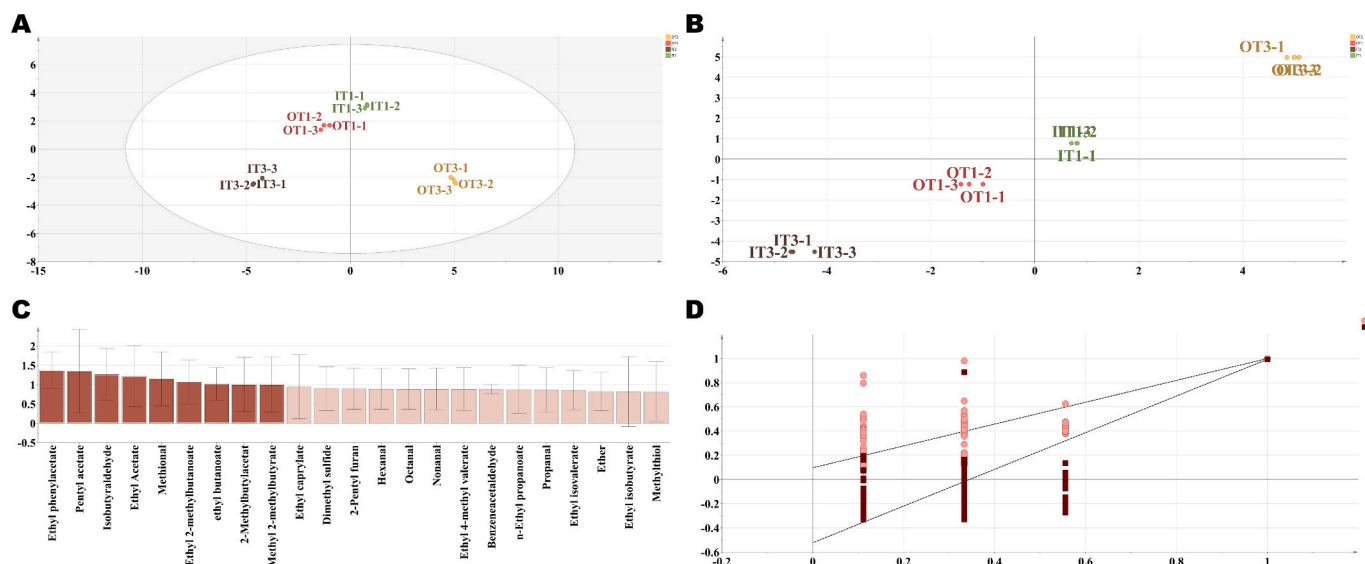
Fig. 6. OPLS-DA model of volatile compounds from different reheating methods.
Note: (a) Scores plot by OPLS-DA, $R^2X = 0.953$, $R^2Y = 0.987$, $Q^2 = 0.978$; (b) Inner relation plot by PLS-DA; (c) VIP scores. Red corresponds to compounds with VIP > 1, and pink represents compounds with VIP < 1. (d) cross-validation plot for the PLS-DA model with 200 calculations in a permutation test: $R^2 = (0.0, 0.168)$, $Q^2 = (0.0, -0.799)$. (For interpretation of the references to color in this figure legend, the reader is referred to the web version of this article.)

fermentation. Fig. 6 (C) shows the variable importance in projection values (VIP) determined using the OPLS-DA model. Compounds with VIP values >1 were considered significant contributors to sample differentiation. Overall, nine compounds were identified with VIP > 1, including seven esters and two aldehydes, namely ethyl phenylacetate, pentyl acetate, isobutyraldehyde, ethyl acetate, methional, ethyl 2-methylbutanoate, ethyl butanoate, 2-methylbutylacetat, and methyl 2-methylbutyrate. Table S3 shows the list of the specific contributions of

these compounds. This highlights that variations in flavor differences due to different fermentation durations and environments are attributed to ester and aldehyde compounds, especially esters. Fig. 6 (D) shows the OPLS-DA permutation test graph, displaying R^2 values of 0.0 and 0.168 and Q^2 values of 0.0 and -0.799. The negative Q^2 value confirms the stability and effectiveness of the model. The intersection points of the regression line Q^2 and Y-axis falling below zero indicate the absence of overfitting.
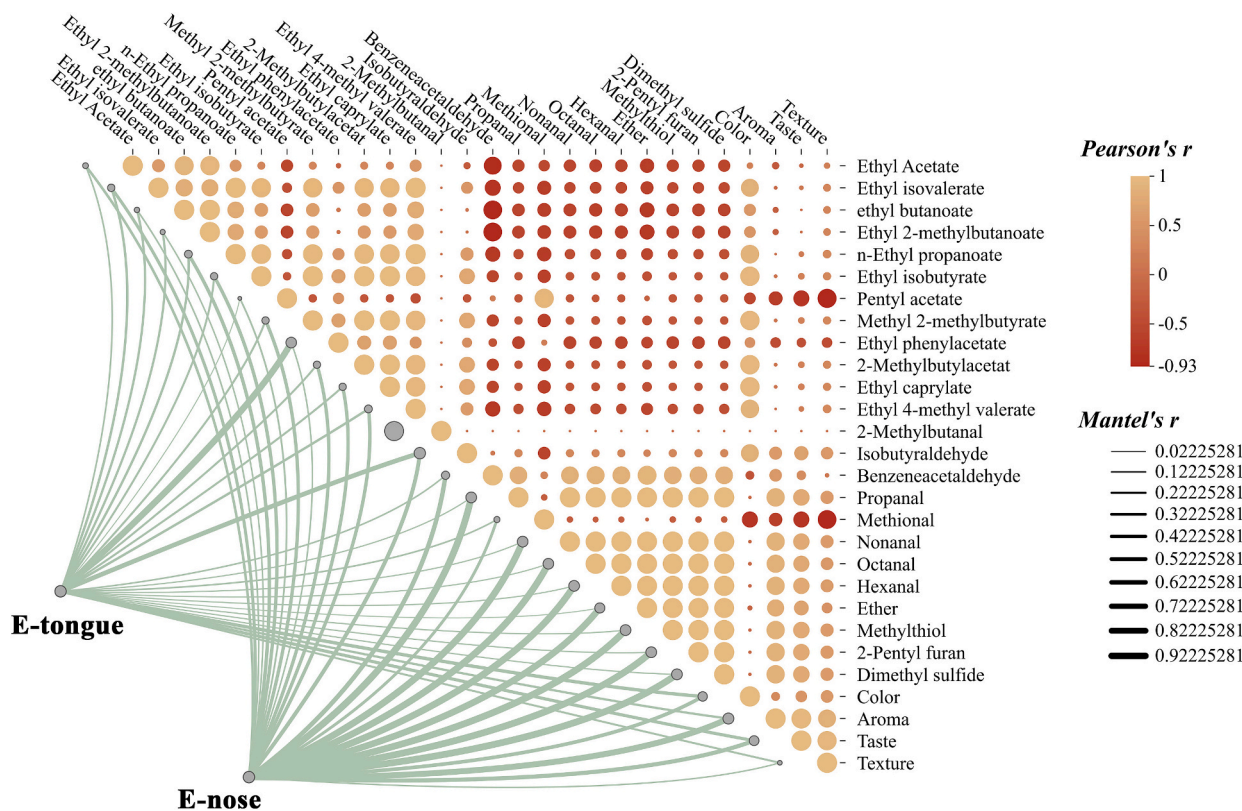
Fig. 7. Analysis of the correlation between sensory properties and volatile organic compounds.

3.9. Correlation between headspace gas chromatography–mass spectrometry, electronic nose, electronic tongue, sensory evaluation

Fig. 7 shows the correlation among HS-GC–MS, *E*-nose, E-tongue, and sensory evaluation using Pearson's and Mantel tests. The Mantel test enables comparison of distance matrix correlations, explaining the correlations between variables. The correlation results reveal robust connections among aroma, taste, color, and VOCs.

In the upper half of the correlation plot, seven esters were observed to positively correlate with color: ethyl isovalerate, n-ethyl propanoate, ethyl isobutyrate, methyl 2-methylbutyrate, 2-methylbutylacetat, ethyl caprylate, ethyl 4-methyl valerate. Conversely, in the lower half, five aldehydes were found to negatively correlate with color but exhibit significant positive correlations with aroma and taste, namely propanal, methional, nonanal, octanal, and hexanal. Additionally, we observed that ether, 2-pentyl furan, and dimethyl sulfide exhibited correlations with aroma and taste. However, despite these positive associations, they maintained negative correlations with color.

We hypothesized that the observed differences in flavor and color between LBBP samples are strongly related to the production mechanisms of aldehydes, heterocyclic compounds, and esters. At low temperatures, esters are typically produced during the fermentation process by microbial communities and yeasts. Their flavors typically exhibit fruity notes. However, due to insufficient temperatures, the Maillard reaction cannot fully occur, thereby diminishing the extent of browning and contributing to the bright reddish-brown color observed in indoor-treated LBBP. In contrast, most aldehydes and heterocyclic compounds are produced through Maillard and Strecker reactions, processes that require higher temperatures. Through these complex chemical processes, LBBP acquires robust nutty, caramel, and roasted flavors, while the elevated temperature leads to its darker brown color. Therefore, future research aimed at improving the color and flavor of LBBP should focus on regulating the Maillard reaction, Strecker reaction, and microbial metabolism. The left part of the plot illustrates the score changes in the r-values of the Mantel test between two matrix variables (*E*-nose and E-tongue). While E-tongue showed only one compound with an r-value >0.85, E-nose exhibited strong correlations with eight compounds, all with r-values >0.95, namely methional, propanal, nonanal, octanal, hexanal, ether, 2-pentyl furan, dimethyl sulfide. This finding aligns with ROAV analysis, indicating that the E-nose can accurately distinguish flavor-contributing substances in LBBP. Consequently, the E-nose can be effective in differentiating the characteristic flavor profiles across various fermentation stages and environments of broad bean pastes.

4. Conclusion

This study examined the flavor profile differences between outdoor- and indoor-fermented LBBP over one- and three-year ripening periods using HS-GC–MS, E-nose, E-tongue, and multivariate statistical analyses. Overall, 95 VOCs were identified in LBBP. Through ROAV combined OPLS-DA, nine characteristic compounds were identified, including seven esters and two aldehydes. Correlation analysis among HS-GC–MS, E-nose, E-tongue, and sensory evaluation results showed aldehydes as the dominant compounds imparting distinctive nutty, caramel, and roasted flavors to outdoor-fermented LBBP, which also exhibited a deeper color than that of indoor-fermented LBBP. Conversely, indoor-fermented LBBP exhibited a fruity flavor predominantly owing to ester compounds, accompanied by a brighter color than that of outdoor-fermented LBBP. The findings from this study provides valuable insights into how ripening time and fermentation environment influence the characteristic flavor profiles of LBBP. The subsequent study will focus on meticulously analyzing the impact of temperature gradients, humidity levels, bacterial species diversity, and salinity concentrations on the flavor of *Linjiangsi* broad bean paste. Additionally, we will use targeted metabolomics combined metagenomics to identify the microbial communities that contribute to its distinctive flavor.

CRediT authorship contribution statement

Chunyuan Ping: Writing – review & editing, Writing – original draft, Data curation, Conceptualization. **Xiaoqing Deng:** Supervision, Funding acquisition. **Ziyuan Guo:** Methodology, Data curation. **Wen Luo:** Supervision. **Xiang Li:** Validation. **Songlin Xin:** Software.

Declaration of competing interest

The authors declare that they have no known competing financial interests or personal relationships that could have appeared influence the work reported in this paper.

Data availability

Data will be made available on request.

Ethical statement

We ensured that participation was entirely voluntary, with no coercion involved. The national laws do not require ethical approval for sensory evaluation. There are no human ethics committees or formal documentation procedures available for sensory evaluation. Comprehensive information about the study's requirements and potential risks was fully disclosed to all participants. Their written consent was obtained before the commencement of the study. We pledged not to release any participant's data without their prior knowledge and consent. Furthermore, participants were given the liberty to withdraw from the study at any point they wished.

Appendix A. Supplementary data

Supplementary data to this article can be found online at https://doi.org/10.1016/j.fochx.2024.101677.

References

Azarbad, M. H., & Jeleń, H. (2014). Determination of hexanal—An indicator of lipid oxidation by static headspace gas chromatography (SHS-GC) in fat-rich food matrices. *Food Analytical Methods, 8*(7), 1727–1733. https://doi.org/10.1007/s12161-014-0043-0

Baldwin, E. A., Bai, J., Plotto, A., & Dea, S. (2011). Electronic noses and tongues: Applications for the food and pharmaceutical industries. *Sensors, 11*(5), 4744–4766. https://doi.org/10.3390/s110504744

Barba, C., Beno, N., Guichard, E., & Thomas-Danguin, T. (2018). Selecting odorant compounds to enhance sweet flavor perception by gas chromatography/olfactometry-associated taste (GC/O-AT). *Food Chemistry, 257*, 172–181. https://doi.org/10.1016/j.foodchem.2018.02.152

Bi, J., Ping, C., Chen, Z., Yang, Z., Li, B., Gao, Y., Zhang, Y., & He, H. (2024). Evaluating the influence of high-temperature sterilization and pasteurization on volatile organic compounds in tomato stewed beef brisket: An analysis using gas chromatography-ion mobility spectrometry and multivariate statistical visualization. *International Journal of Gastronomy and Food Science, 100939*. https://doi.org/10.1016/j.ijgfs.2024.100939

Bleicher, J., Ebner, E. E., & Bak, K. H. (2022). Formation and analysis of volatile and odor compounds in meat—A review. *Molecules, 27*(19), 6703. https://doi.org/10.3390/molecules27196703

Deng, Y., Wang, R., Zhang, Y., Li, X., Gooneratne, R., & Li, J. (2022). Comparative analysis of flavor, taste, and volatile organic compounds in opossum shrimp paste during long-term natural fermentation using e-nose, e-tongue, and HS-SPME-GC-MS. *Foods, 11*(13), 1938. https://doi.org/10.3390/foods11131938

Devanthi, P. V. P., & Gkatzionis, K. (2019). Soy sauce fermentation: Microorganisms, aroma formation, and process modification. *Food Research International, 120*, 364–374. https://doi.org/10.1016/j.foodres.2019.03.010

Diez-Simon, C., Eichelsheim, C., Mumm, R., & Hall, R. D. (2020). Chemical and sensory characteristics of soy sauce: A review. *Journal of Agricultural and Food Chemistry, 68* (42), 11612–11630. https://doi.org/10.1021/acs.jafc.0c04274

Feng, Y., Xie, Z., Huang, M., Tong, X., Hou, S., Tin, H., & Zhao, M. (2024). Decoding temperature-driven microbial community changes and flavor regulation mechanism during winter fermentation of soy sauce. *Food Research International, 177*, Article 113756. https://doi.org/10.1016/j.foodres.2023.113756

Gao, L., Liu, T., An, X., Zhang, J., Ma, X., & Cui, J. (2017). Analysis of volatile flavor compounds influencing Chinese-type soy sauces using GC–MS combined with HS-SPME and discrimination with electronic nose. *Journal of Food Science and Technology, 54*, 130–143. https://doi.org/10.1007/s13197-016-2444-0

Jiang, S., Wang, X., Yu, M., Tian, J., Chang, P., & Zhu, S. (2023). Bitter peptides in fermented soybean foods-a review. *Plant Foods for Human Nutrition, 78*(2), 261–269. https://doi.org/10.1007/s11130-023-01077-3

Jung, H. Y., Kwak, H. S., Kim, M. J., Kim, Y., Kim, K. O., & Kim, S. S. (2017). Comparison of a descriptive analysis and instrumental measurements (electronic nose and electronic tongue) for the sensory profiling of Korean fermented soybean paste (doenjang). *Journal of Sensory Studies, 32*(5), Article e12282. https://doi.org/10.1111/joss.12282

Li, F., Wang, Y., Liao, H., Long, Y., Yu, Q., Xie, J., & Chen, Y. (2024). Exploring correlations between soy sauce components and the formation of thermal contaminants during low-salt solid-state fermentation. *Food Research International, 114113*. https://doi.org/10.1016/j.foodres.2024.114113

Li, X., Zhao, C., Zheng, C., Liu, J., Vu, V. H., Wang, X., & Sun, Q. (2017). Characteristics of microbial community and aroma compounds in traditional fermentation of Pixian broad bean paste as compared to industrial fermentation. *International Journal of Food Properties, 20*(sup3), S2520–S2531. https://doi.org/10.1080/10942912.2017.1373358

Li, Y. H., Wang, H. R., Meng, Y. Y., Zhao, W., Tan, L. J., Liu, H. Q., … Zhao, Y. (2022). Recent Progress in the ripening mechanism of ready-to-eat fermented meat products. *Food. Science, 43*(09), 337–345. https://doi.org/10.7506/spkx1002-6630-20210506-034

Li, Z., Dong, L., Huang, Q., & Wang, X. (2016). Bacterial communities and volatile compounds in Doubanjiang, a Chinese traditional red pepper paste. *Journal of Applied Microbiology, 120*(6), 1585–1594. https://doi.org/10.1111/jam.13130

Lin, L., Zeng, J., Tian, Q., Ding, X., Zhang, X., & Gao, X. (2022). Effect of the bacterial community on the volatile flavour profile of a Chinese fermented condiment – Red sour soup – During fermentation. *Food Research International, 155*, Article 111059. https://doi.org/10.1016/j.foodres.2022.111059

Lin, P., Fu, G. M., Wu, S. M., Zeng, T. T., Zhu, Y. F., Liu, X. Q., … Hong, L. X. (2022). Effect of Rice processing and quality on the fermentation indexes and base liquor quality of Texiang baijiu. *Liquor-making science & Technology, 03*, 65–70. https://doi.org/10.13746/j.njkj.2021150

Liu, P., Xiang, Q., Sun, W., Wang, X., Lin, J., Che, Z., & Ma, P. (2020). Correlation between microbial communities and key flavors during post-fermentation of Pixian broad bean paste. *Food Research International, 137*, Article 109513. https://doi.org/10.1016/j.foodres.2020.109513

Lu, Y., Tan, X., Lv, Y., Yang, G., Chi, Y., & He, Q. (2020). Flavor volatiles evolution of Chinese horse bean-chili-paste during ripening, accessed by GC× GC-TOF/MS and GC-MS-olfactometry. *International Journal of Food Properties, 23*(1), 570–581. https://doi.org/10.1080/10942912.2020.1749066

Luo, J., Nasiru, M. M., Zhuang, H., Zhou, G., & Zhang, J. (2021). Effects of partial NaCl substitution with high-temperature ripening on proteolysis and volatile compounds during process of Chinese dry-cured lamb ham. *Food Research International, 140*, Article 110001. https://doi.org/10.1016/j.foodres.2020.110001

Lv, Y. C., Song, H. L., Li, X., Wu, L., & Guo, S. T. (2011). Influence of blanching and grinding process with hot water on beany and non-beany flavor in soymilk. *Journal of Food Science, 76*(1), S20–S25. https://doi.org/10.1111/j.1750-3841.2010.01947.x

Ma, R., Shen, H., Cheng, H., Zhang, G., & Zheng, J. (2023). Combining e-nose and e-tongue for improved recognition of instant starch noodles seasonings. *Frontiers in Nutrition, 9*, 1074958. https://doi.org/10.3389/fnut.2022.1074958

Manzocco, L., Plazzotta, S., Maifreni, M., Calligaris, S., Anese, M., & Nicoli, M. C. (2016). Impact of UV-C light on storage quality of fresh-cut pineapple in two different packages. *LWT-Food Science and Technology, 65*, 1138–1143. https://doi.org/10.1016/j.lwt.2015.10.007

Millena, C. G., Balonzo, A. R. R., Rentoy, J. R., Ruivivar, S. S., & Bobiles, S. C. (2023). Effect of fermentation stages on the nutritional and mineral bioavailability of cacao beans (*Theobroma cacao L*). *Journal of Food Composition and Analysis, 115*, Article 104886. https://doi.org/10.1016/j.jfca.2022.104886

Olivares, A., Navarro, J. L., & Flores, M. (2011). Effect of fat content on aroma generation during processing of dry fermented sausages. *Meat Science, 87*(3), 264–273. https://doi.org/10.1016/j.meatsci.2010.10.021

Pei, L., Liu, W., Jiang, L., Xu, H., Liu, L., Wang, X., Liu, M., Abudureheman, B., Zhang, H., & Chen, J. (2023). Effect of high hydrostatic pressure on aroma volatile compounds and aroma precursors of Hami melon juice. *Frontiers in Nutrition, 10*. https://doi.org/10.3389/fnut.2023.1285590

Que, Z., Jin, Y., Huang, J., Zhou, R., & Wu, C. (2023). Flavor compounds of traditional fermented bean condiments: Classes, synthesis, and factors involved in flavor formation. *Trends in Food Science & Technology, 133*, 160–175. https://doi.org/10.1016/j.tifs.2023.01.010

Rai, A. K., Sanjukta, S., & Jeyaram, K. (2017). Production of angiotensin I converting enzyme inhibitory (ACE-I) peptides during milk fermentation and their role in reducing hypertension. *Critical Reviews in Food Science and Nutrition, 57*(13), 2789–2800. https://doi.org/10.1080/10408398.2015.1068736

Sanderson, G. W., & Grahamm, H. N. (1973). Formation of black tea aroma. *Journal of Agricultural and Food Chemistry, 21*(4), 576–585. https://doi.org/10.1021/jf60188a007

Sanjukta, S., & Rai, A. K. (2016). Production of bioactive peptides during soybean fermentation and their potential health benefits. *Trends in Food Science & Technology, 50*, 1–10. https://doi.org/10.1016/j.tifs.2016.01.010

Seo, S. H., Park, S. E., Kim, E. J., Lee, K. I., Na, C. S., & Son, H. S. (2018). A GC-MS based metabolomics approach to determine the effect of salinity on kimchi. *Food Research International, 105*, 492–498. https://doi.org/10.1016/j.foodres.2017.11.069

Smit, B. A., Engels, W. J., & Smit, G. (2009). Branched chain aldehydes: Production and breakdown pathways and relevance for flavour in foods. *Applied Microbiology and Biotechnology, 81*, 987–999. https://doi.org/10.1007/s00253-008-1758-x

Starowicz, M., & Zieliński, H. (2019). How Maillard reaction influences sensorial properties (color, flavor and texture) of food products? *Food Reviews International, 35* (8), 707–725. https://doi.org/10.1080/87559129.2019.1600538

Steinhaus, P., & Schieberle, P. (2007). Characterization of the key aroma compounds in soy sauce using approaches of molecular sensory science. *Journal of Agricultural and Food Chemistry, 55*(15), 6262–6269. https://doi.org/10.1021/jf0709092

Tang, J., Robichaux, M. A., Wu, K., Pei, J., Nguyen, N. T., Zhou, Y., … Xiao, H. (2019). Single-atom fluorescence switch: A general approach toward visible-light-activated dyes for biological imaging. *Journal of the American Chemical Society, 141*(37), 14699–14706. https://doi.org/10.1021/jacs.9b06237

Tian, H., Xiong, J., Yu, H., Chen, C., & Lou, X. (2023). Flavor optimization in dairy fermentation: From strain screening and metabolic diversity to aroma regulation. *Trends in Food Science & Technology, 141*, Article 104194. https://doi.org/10.1016/j.tifs.2023.104194

Wang, Y., Gao, Y., Liang, W., Liu, Y., & Gao, H. (2020). Identification and analysis of the flavor characteristics of unfermented stinky tofu brine during fermentation using SPME-GC–MS, e-nose, and sensory evaluation. *Journal of Food Measurement and Characterization, 14*(1), 597–612. https://doi.org/10.1007/s11694-019-00351-w

Wei, G., Chitrakar, B., Regenstein, J. M., Sang, Y., & Zhou, P. (2023). Microbiology, flavor formation, and bioactivity of fermented soybean curd (furu): A review. *Food Research International, 163*, Article 112183. https://doi.org/10.1016/j.foodres.2022.112183

Ye, T., Liu, J., Wan, P., Liu, S., Wang, Q., & Chen, D. (2022). Investigation of the effect of polar components in cream on the flavor of heated cream based on NMR and GC-MS methods. *LWT-Food Science and Technology, 155*, Article 112940. https://doi.org/10.1016/j.lwt.2021.112940

Yıltırak, S., Kocadağlı, T., Çelik, E. E., Kanmaz, E.Ö., & Gökmen, V. (2022). Effects of sprouting and fermentation on the formation of Maillard reaction products in different cereals heated as wholemeal. *Food Chemistry, 389*, Article 133075. https://doi.org/10.1016/j.foodchem.2022.133075

Yu, S., Huang, X., Wang, L., Ren, Y., Zhang, X., & Wang, Y. (2022). Characterization of selected Chinese soybean paste based on flavor profiles using HS-SPME-GC/MS, E-nose and E-tongue combined with chemometrics. *Food Chemistry, 375*, Article 131840. https://doi.org/10.1016/j.foodchem.2021.131840

Zhang, J., Sun, H., Chen, S., Zeng, L., & Wang, T. (2017). Anti-fungal activity, mechanism studies on α-Phellandrene and nonanal against Penicillium cyclopium. *Botanical Studies, 58*(1), 1–9. https://doi.org/10.1186/s40529-017-0168-8

Zhang, K., Zhang, T., Guo, R., Ye, Q., Zhao, H., & Huang, X. (2023). The regulation of key flavor of traditional fermented food by microbial metabolism: A review. *Food Chemistry. X, 19*, Article 100871. https://doi.org/10.1016/j.fochx.2023.100871

Zhao, S., Niu, C., Suo, J., Zan, Y., Wei, Y., Zheng, F., Liu, C., Wang, J., & Li, Q. (2021). Unraveling the mystery of 'bask in daytime and dewed at night' technique in doubanjiang (broad bean paste) fermentation. *LWT-Food Science and Technology, 149*, Article 111723. https://doi.org/10.1016/j.lwt.2021.111723

Zhao, S., Niu, C., Yang, X., Xu, X., Zheng, F., Liu, C., Wang, J., & Li, Q. (2022). Roles of sunlight exposure on chemosensory characteristic of broad bean paste by untargeted profiling of volatile flavors and multivariate statistical analysis. *Food Chemistry, 381*, Article 132115. https://doi.org/10.1016/j.foodchem.2022.132115

Zhu, J., Wang, J., Yuan, H., Ouyang, W., Li, J., Hua, J., & Jiang, Y. (2022). Effects of fermentation temperature and time on the color attributes and tea pigments of Yunnan congou black tea. *Foods, 11*(13), 1845. https://doi.org/10.3390/foods11131845